

# <sup>1</sup> eo-tides: Tide modelling tools for large-scale satellite Earth observation analysis

<sup>3</sup> **Robbi Bishop-Taylor**  <sup>1</sup>¶, **Claire Phillips**  <sup>1</sup>, **Stephen Sagar**  <sup>1</sup>, **Vanessa Newey**<sup>1</sup>, and **Tyler Sutterley**  <sup>2</sup>

<sup>5</sup> 1 Geoscience Australia, Australia  <sup>2</sup> University of Washington Applied Physics Laboratory, United States of America  ¶ Corresponding author

DOI: [10.xxxxxx/draft](https://doi.org/10.xxxxxx/draft)

## Software

- [Review](#) ↗
- [Repository](#) ↗
- [Archive](#) ↗

Editor: [Open Journals](#) ↗

Reviewers:

- [@openjournals](#)

Submitted: 01 January 1970

Published: unpublished

## License

Authors of papers retain copyright and release the work under a Creative Commons Attribution 4.0 International License ([CC BY 4.0](#)).  
eo-tides tools can be applied to petabytes of freely available satellite data loaded from the cloud using Open Data Cube (ODC)’s odc-stac or datacube packages (e.g. using [Digital Earth Australia](#) or [Microsoft Planetary Computer’s STAC SpatioTemporal Asset Catalogues](#)). Additional functionality allows users to assess potential satellite-tide biases and validate modelled tides with external tide gauge data — critical considerations for ensuring the reliability and accuracy of coastal EO workflows. These open-source tools support the efficient, scalable and robust analysis of coastal EO data for any time period or location globally.

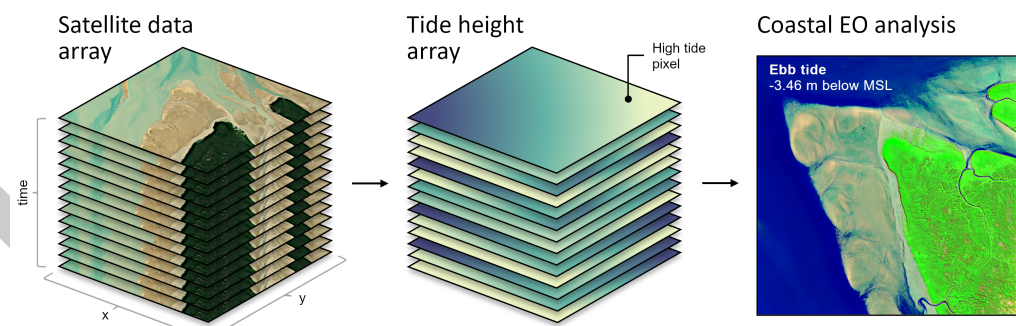


**Figure 1:** A typical eo-tides coastal EO workflow, with tide heights modelled into every pixel in a spatio-temporal stack of satellite data (for example, from ESA’s Sentinel-2 or NASA/USGS Landsat), then combined to derive insights into dynamic coastal environments.

## <sup>24</sup> Statement of need

<sup>25</sup> Satellite remote sensing offers an unparalleled resource for examining dynamic coastal environments through time or across large regions (Turner et al., 2021; Vitousek et al., 2023).  
<sup>26</sup> However, the highly variable influence of ocean tides can complicate analyses, making it difficult  
<sup>27</sup> to separate the influence of changing tides from patterns of true coastal change (Vos et al.,  
<sup>28</sup> 2019). This is a particularly challenging for large-scale coastal EO analyses, where failing to  
<sup>29</sup> account for tide dynamics can lead to inaccurate or misleading insights into satellite-observed  
<sup>30</sup> coastal processes.  
<sup>31</sup>

<sup>32</sup> Conversely, information about ocean tides can provide unique environmental insights that can  
<sup>33</sup> significantly enhance the value of EO data. Traditionally, satellite data dimensions include  
<sup>34</sup> the geographic “where” and temporal “when” of acquisition. Introducing tide height as an  
<sup>35</sup> additional analysis dimension allows data to be filtered, sorted, and analysed based on tidal  
<sup>36</sup> dynamics, offering a transformative re-imagining of traditional multi-temporal EO analysis  
<sup>37</sup> (Sagar et al., 2017). For instance, satellite data can be analysed to focus on ecologically  
<sup>38</sup> significant tidal stages (e.g., high tide, low tide, spring or neap tides) or specific tidal processes  
<sup>39</sup> (e.g., ebb or flow tides; Sent et al. (2025)).

<sup>40</sup> This concept has been used to map coastal change at continental-scale (Bishop-Taylor et al.,  
<sup>41</sup> 2021), map intertidal zone extent and elevation (Bishop-Taylor et al., 2019; Murray et al.,  
<sup>42</sup> 2012; Sagar et al., 2017), and creating tidally-constrained coastal image composites (Sagar  
<sup>43</sup> et al., 2018). However, these methods have traditionally relied on bespoke, closed-source, or  
<sup>44</sup> difficult-to-install tide modeling tools, limiting their reproducibility and portability. To support  
<sup>45</sup> the next generation of coastal EO workflows, there is a pressing need for efficient open-source  
<sup>46</sup> tools for combining satellite data with tide modeling. eo-tides addresses this need through  
<sup>47</sup> functionality offered in five main analysis modules (utils, model, eo, stats, validation)  
<sup>48</sup> described below.

## <sup>49</sup> Features

### <sup>50</sup> Setting up tide models

<sup>51</sup> The `eo_tides.utils` module simplifies the setup of ocean tide models, addressing a common  
<sup>52</sup> barrier to coastal EO workflows. Tools like `list_models` provide feedback on available and  
<sup>53</sup> supported models (Figure 2), while `clip_models` can improve performance by clipping large  
<sup>54</sup> model files to smaller regions, significantly reducing processing times for high-resolution models  
<sup>55</sup> like FES2022. Comprehensive documentation is available to assist setting up commonly used  
<sup>56</sup> tide models, including downloading and organising model files.

	Model	Expected path
	EOT20	tide_models/EOT20/ocean_tides
	FES2014	tide_models/fes2014/ocean_tide
	HAMTIDE11	tide_models/hamtide
...	...	...

Summary:  
Available models: 2/50

**Figure 2:** An example output from `list_tides`, providing a useful summary table that clearly identifies available and supported tide models.

## 57 Modelling tides

58 The `eo_tides.model` module is powered by tide modelling functionality from the pyTMD Python  
 59 package ([Sutterley et al., 2017](#)).

60 pyTMD is an open-source tidal prediction software that simplifies the calculation of ocean  
 61 and earth tides. Tides are frequently decomposed into harmonic constants (or constituents)  
 62 associated with the relative positions of the sun, moon and Earth. pyTMD.io contains routines  
 63 for reading and spatially interpolating major constituent values from commonly available ocean  
 64 tide models. pyTMD.astro contains routines for computing the positions of celestial bodies for  
 65 a given time. For ocean tides, pyTMD computes the longitudes of the sun (S), moon (H), lunar  
 66 perigee (P), ascending lunar node (N) and solar perigee (PP). pyTMD.arguments combines  
 67 astronomical coefficients with the “Doodson number” of each constituent, and adjusts the  
 68 amplitude and phase of each constituent based on their modulations over the 18.6 year nodal  
 69 period. Finally, pyTMD.predict uses results from those underlying functions to predict tidal  
 70 values at a given location and time.

71 The `model_tides` function from `eo_tides.model` wraps pyTMD functionality to return tide  
 72 predictions in a standardised pandas.DataFrame format, enabling integration with satellite  
 73 EO data and parallelised processing for improved performance. Parallelisation in eo-tides is  
 74 automatically optimised based on available workers and requested tide models and tide modelling  
 75 locations. This parallelisation can significantly improve performance, especially for large-scale  
 76 analyses run on multi-core machines ([Table 1](#)). Additional functions like `model_phases` classify  
 77 tides into high/low/flow/ebb phases, critical for interpreting satellite-observed coastal processes  
 78 like changing turbidity and ocean colour ([Sent et al., 2025](#)).

**Table 1:** A [benchmark comparison](#) of tide modelling performance with parallelisation on vs. off, for a typical large-scale analysis involving a month of hourly tides modelled at 10,000 point locations using three models (FES2022, TPXO10, GOT5.6).

Cores	Parallelisation	No parallelisation	Speedup
8	2min 46s ± 663 ms	9min 28s ± 536 ms	3.4x
32	55.9 s ± 560 ms	9min 24s ± 749 ms	10.1x

## 79 Combining tides with satellite data

80 The `eo_tides.eo` module integrates modelled tides with xarray-format satellite data. eo-tides  
 81 offers two tide attribution approaches that differ in complexity and performance: `tag_tides`  
 82 assigns a single tide height per timestep for small-scale studies, while `pixel_tides` models  
 83 tides spatially and temporally for larger-scale analyses, returning a unique tide height for each  
 84 pixel in a dataset ([Table 2](#), [Figure 3](#)). These functions can be applied to satellite data for any  
 85 coastal location on the planet, for example using open data loaded from the cloud using [ODC](#)  
 86 and STAC ([STAC contributors, 2024](#)).

**Table 2:** Comparison of the `tag_tides` and `pixel_tides` functions.

<code>tag_tides</code>	<code>pixel_tides</code>
<ul style="list-style-type: none"> <li>- Assigns a single tide height to each satellite image timestep</li> <li>- Single tide height per image can produce artefacts and discontinuities</li> <li>- Fast, low memory use</li> <li>- Ideal for local or site-scale analysis</li> </ul>	<ul style="list-style-type: none"> <li>- Assigns a tide height to every individual pixel through time to capture spatial tide dynamics</li> <li>- Produce spatially seamless results across large regions</li> <li>- Slower, higher memory use</li> <li>- Ideal for large-scale coastal product generation</li> </ul>

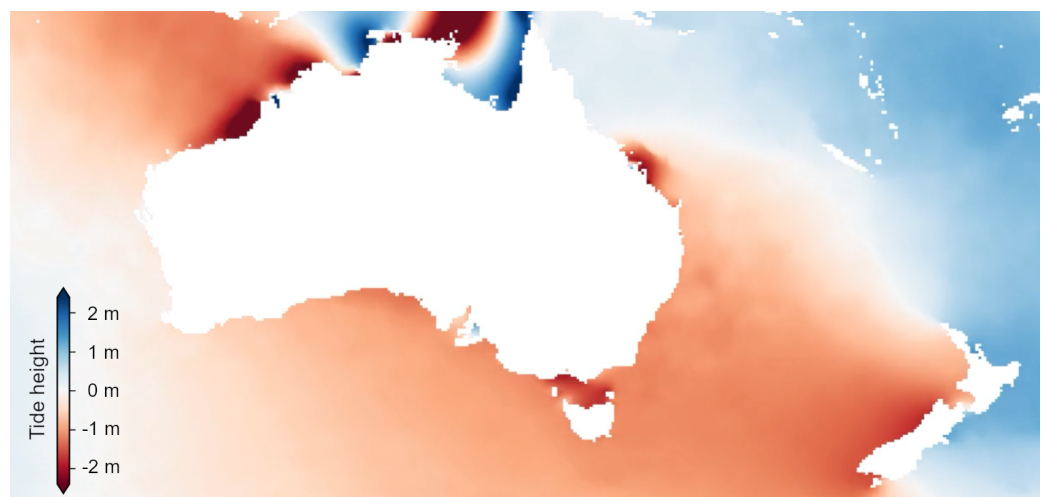


**Figure 3:** An example spatial tide height output produced by the `pixel_tides` function.

### 87 Calculating tide statistics and satellite biases

88 The `eo_tides.stats` module identifies biases caused by complex tide aliasing interactions  
 89 between tidal dynamics and satellite observations. These interactions can prevent satellites  
 90 from observing the entire tide cycle (Eleveld et al., 2014; Sent et al., 2025), leading coastal EO  
 91 studies to produce biased or misleading results (Bishop-Taylor et al., 2019). The `tide_stats`  
 92 and `pixel_stats` functions produce a range of useful automated reports, plots and statistics  
 93 that summarise how well a satellite time series captures real-world tidal conditions (Figure 4).

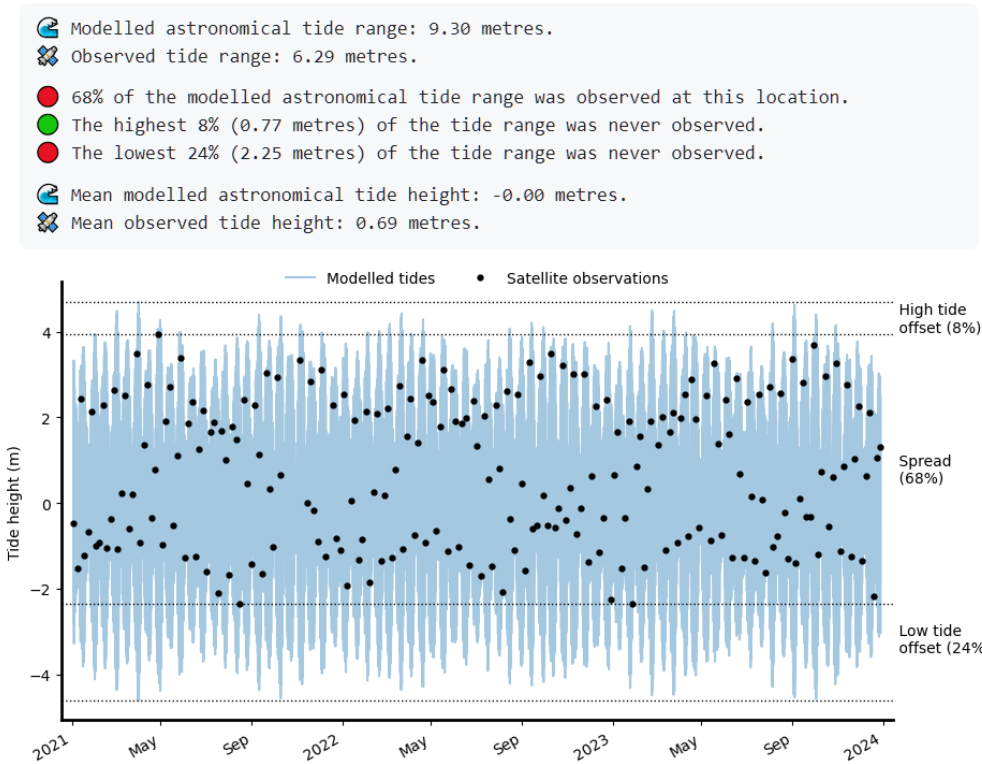


**Figure 4:** An example of tidally-biased satellite coverage, where only ~68% of the modelled astronomical tide range is observed.

## 94     Validating modelled tides

95     The `eo_tides.validation` module validates modelled tides against sea-level measurements  
 96     from the GESLA Global Extreme Sea Level Analysis (Haigh et al., 2023) archive (Figure 5).  
 97     It enables comparison of multiple tide models against observed data, allowing users to select  
 98     optimal tide models for their specific study area or application (Figure 5).

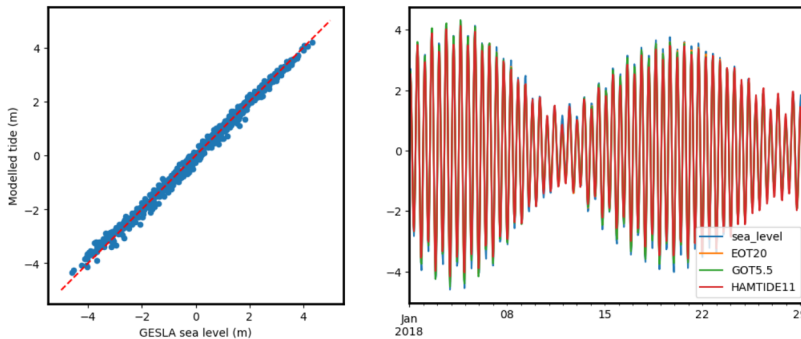


Figure 5: A comparison of multiple tide models (EOT20, GOT5.5, HAMTIDE11) against observed sea level data from the Broome 62650 GESLA tide gauge.

## 99     Research projects

100    Early versions of `eo-tides` functions have been used for continental-scale intertidal mapping  
 101    (Bishop-Taylor et al., 2024), multi-decadal shoreline mapping across Australia (Bishop-Taylor  
 102    et al., 2021) and Africa, and for satellite-derived shoreline tide correction in the CoastSeg  
 103    Python package (Fitzpatrick et al., 2024).

## 104    Acknowledgements

105    Functions from `eo-tides` were originally developed in the Digital Earth Australia Notebooks  
 106    and Tools repository (Krause et al., 2021). We thank all DEA Notebooks contributors for  
 107    their invaluable assistance with code review, feature suggestions and code edits. This paper is  
 108    published with the permission of the Chief Executive Officer, Geoscience Australia (copyright  
 109    2025).

## 110    References

- 111    Bishop-Taylor, R., Nanson, R., Sagar, S., & Lymburner, L. (2021). Mapping Australia's  
       Dynamic Coastline at Mean Sea Level using Three Decades of Landsat Imagery. *Remote  
       Sensing of Environment*, 267, 112734. <https://doi.org/10.1016/j.rse.2021.112734>
- 114    Bishop-Taylor, R., Phillips, C., Newey, V., & Sagar, S. (2024). *Digital Earth Australia Intertidal*.  
       Commonwealth of Australia (Geoscience Australia). <https://doi.org/10.26186/149403>
- 116    Bishop-Taylor, R., Sagar, S., Lymburner, L., & Beaman, R. J. (2019). Between the tides:  
       Modelling the elevation of australia's exposed intertidal zone at continental scale. *Estuarine,  
       Coastal and Shelf Science*, 223, 115–128. <https://doi.org/10.1016/j.ecss.2019.03.006>
- 119    Elefeld, M. A., Van der Wal, D., & Van Kessel, T. (2014). Estuarine suspended parti-  
       culate matter concentrations from sun-synchronous satellite remote sensing: Tidal  
       and meteorological effects and biases. *Remote Sensing of Environment*, 143, 204–215.  
       <https://doi.org/10.1016/j.rse.2013.12.019>

- 123 Fitzpatrick, S., Buscombe, D., Warrick, J. A., Lundine, M. A., & Vos, K. (2024). CoastSeg: An  
 124 accessible and extendable hub for satellite-derived-shoreline (SDS) detection and mapping.  
 125 *Journal of Open Source Software*, 9(99), 6683. <https://doi.org/10.21105/joss.06683>
- 126 Haigh, I. D., Marcos, M., Talke, S. A., Woodworth, P. L., Hunter, J. R., Hague, B. S.,  
 127 Arns, A., Bradshaw, E., & Thompson, P. (2023). GESLA version 3: A major update to  
 128 the global higher-frequency sea-level dataset. *Geoscience Data Journal*, 10(3), 293–314.  
 129 <https://doi.org/10.1002/gdj3.174>
- 130 Hoyer, S., & Joseph, H. (2017). xarray: N-d labeled arrays and datasets in python. *Journal of  
 131 Open Research Software*, 5(1). <https://doi.org/10.5334/jors.148>
- 132 Krause, C., Dunn, B., Bishop-Taylor, R., Adams, C., Burton, C., Alger, M., Chua, S., Phillips, C.,  
 133 Newey, V., Kouzoubov, K., Leith, A., Ayers, D., & Hicks, A. (2021). *Digital Earth Australia  
 134 notebooks and tools repository*. <https://github.com/GeoscienceAustralia/dea-notebooks/>;  
 135 Commonwealth of Australia (Geoscience Australia). <https://doi.org/10.26186/145234>
- 136 McKinney, Wes. (2010). Data Structures for Statistical Computing in Python. In Stéfan van  
 137 der Walt & Jarrod Millman (Eds.), *Proceedings of the 9th Python in Science Conference*  
 138 (pp. 56–61). <https://doi.org/10.25080/Majora-92bf1922-00a>
- 139 Murray, N. J., Phinn, S. R., Clemens, R. S., Roelfsema, C. M., & Fuller, R. A. (2012).  
 140 Continental scale mapping of tidal flats across east asia using the landsat archive. *Remote  
 141 Sensing*, 4(11), 3417–3426. <https://doi.org/10.3390/rs4113417>
- 142 odc-geo contributors. (2024). Opendatacube/odc-geo. In *Github repository*. GitHub.  
 143 <https://github.com/opendatacube/odc-geo>
- 144 pandas development team. (2020). Pandas-dev/pandas: pandas (latest). Zenodo. <https://doi.org/10.5281/zenodo.3509134>
- 146 Sagar, S., Phillips, C., Bala, B., Roberts, D., Lymburner, L., & Beaman, R. J. (2018).  
 147 Generating continental scale pixel-based surface reflectance composites in coastal regions  
 148 with the use of a multi-resolution tidal model. *Remote Sensing*, 10(3), 480. <https://doi.org/10.3390/rs10030480>
- 150 Sagar, S., Roberts, D., Bala, B., & Lymburner, L. (2017). Extracting the intertidal extent and  
 151 topography of the australian coastline from a 28 year time series of landsat observations.  
 152 *Remote Sensing of Environment*, 195, 153–169. <https://doi.org/10.1016/j.rse.2017.04.009>
- 153 Sent, G., Antunes, C., Spyrikos, E., Jackson, T., Atwood, E. C., & Brito, A. C. (2025). What  
 154 time is the tide? The importance of tides for ocean colour applications to estuaries. *Remote  
 155 Sensing Applications: Society and Environment*, 37, 101425. <https://doi.org/10.2139/ssrn.4858713>
- 157 STAC contributors. (2024). SpatioTemporal Asset Catalog (STAC) specification. <https://stacspec.org>
- 159 Sutterley, T. C., Alley, K., Brunt, K., Howard, S., Padman, L., & Siegried, M. (2017). pyTMD:  
 160 Python-based tidal prediction software. Zenodo. <https://doi.org/10.5281/zenodo.5555395>
- 161 Turner, I. L., Harley, M. D., Almar, R., & Bergsma, E. W. J. (2021). Satellite optical imagery  
 162 in Coastal Engineering. *Coastal Engineering*, 167, 103919. <https://doi.org/10.1016/j.coastaleng.2021.103919>
- 164 Vitousek, S., Buscombe, D., Vos, K., Barnard, P. L., Ritchie, A. C., & Warrick, J. A. (2023).  
 165 The future of coastal monitoring through satellite remote sensing. *Cambridge Prisms:  
 166 Coastal Futures*, 1, e10. <https://doi.org/10.1017/cft.2022.4>
- 167 Vos, K., Splinter, K. D., Harley, M. D., Simmons, J. A., & Turner, I. L. (2019). CoastSat: A  
 168 Google Earth Engine-enabled Python toolkit to extract shorelines from publicly available  
 169 satellite imagery. *Environmental Modelling & Software*, 122, 104528. <https://doi.org/10.1016/j.envsoft.2019.104528>

DRAFT